Available online at www.sciencedirect.com
SCIENCE DIRECT
Remote Sensing of Environment 100 (2006) 335 – 347
Remote Sensing of Environment
www.elsevier.com/locate/rse

Modeling the interaction of infrared radiation (750 to 2500 nm) with bifacial and unifacial plant leaves

Gladimir V.G. Baranoski *

University of Waterloo, School of Computer Science, Natural Phenomena Simulation Group 200 University Avenue West Waterloo, Ontario Canada N2L 3G1

Received 30 April 2005; received in revised form 25 October 2005; accepted 29 October 2005

Abstract

Plants are arguably among the most investigated remote sensing targets. Due to their economical and environmental importance, several models to simulate radiation transport and absorption by foliar tissues have been proposed in remote sensing and related fields. The main goal of this research is to present alternative modeling strategies for the investigation of these phenomena. These solutions consist in algorithmic models specifically designed to simulate the interaction of radiation with bifacial and unifacial plant leaves. Their flexible formulations based on standard Monte Carlo techniques make their implementation straightforward and allow their use in investigations involving different regions of the electromagnetic spectrum of radiation. In this paper, they are examined in the context of infrared applications. This choice is motivated by the simulation challenges posed by the processes that relate biophysical characteristics to optical properties of plant leaves in this domain. The accuracy and predictability of the proposed models have been evaluated through comparisons between modeled results and measured data. The results of these evaluations illustrate the applicability of the proposed models to investigations involving the predictive simulation of foliar spectral signatures.

Keywords: Infrared radiation; Absorption; Scattering; Reflectance; Transmittance; BRDF; BTDF; Plants; Foliar tissues

1. Introduction

Plants represent a natural resource on which all human and animal life depends. During the last decades, they have become one of the primary targets of remote sensing research (e.g., projects oriented towards ecology (Hobbs, 1990; Merzlyak et al., 2002), agriculture (Chelle, 2005; Clevers, 1994) and forestry (Horler & Barber, 1981)). More recently, they have also become object of space research (e.g., projects investigating the role of plants in providing life support during long space missions such as voyages to Mars (Salisbury et al., 2002), and projects aiming at detecting clues to alien life using infrared reflectance signatures, "red edge" (Arnold et al., 2002; Seager et al., 2005)). In order to strengthen the scientific basis required for these applications, it is necessary to extend the current understanding of the biophysical processes involved in the interaction of radiation with foliar tissues. We believe that the gathering of reliable data and the development of predictive models to investigate these phenomena are essential to achieve this goal.

Most of the available models of radiation interaction with plant leaves have been developed by the remote sensing community, and different simulation approaches, such as the application of Kubelka–Munk theory and Monte Carlo methods, have been employed in their design. Although a thorough examination of these models is beyond the scope of this work (we refer the interested reader to the texts by Jacquemoud and Ustin (2001) and Baranoski and Rokne (2004)), it is important to note that these models are primarily designed to provide spectral power distributions given in terms of absolute reflectance and transmittance values which, in turn, can be used in inversion procedures (Brakke et al., 1996; Verstraete, 1994). Spatial power distributions given in terms of a leaf's BDF (bidirectional scattering distribution function) or its components, namely BRDF (bidirectional reflectance distribution function) and BTDF (bidirectional transmittance distribution function) (Nicodemus et al., 1992), are usually not explicitly computed by most models.

There are, however, comprehensive biophysically based models that can provide both spectral and spatial quantities

* Fax: +1 519 8851208.
E-mail address: gvgbaran@curumin.math.uwaterloo.ca.

0034-4257/$ - see front matter © 2005 Elsevier Inc. All rights reserved.
doi:10.1016/j.rse.2005.10.015

with respect to the radiation propagated by a plant leaf. The Monte Carlo ray tracing based model developed by Govaerts et al. (1996), RAYTRAN, and the algorithmic BDF model developed by Baranoski and Rokne (1997), ABM, are examples of such models. Both models simulate the propagation of light in a typical bifacial dicotyledon leaf using Monte Carlo methods, which can provide a flexible approach to the modeling of light transport in organic tissues. These models, however, use different levels of abstraction to represent the foliar tissues.

The RAYTRAN model, which was developed primarily for remote sensing applications, takes into account the explicit modeling of the three-dimensional internal cellular structure of various leaf tissues (Jacquemoud et al., 1997). Such detailed description of foliar internal tissues leads to accurate results provided that reliable input data is available. However, in order to account for changes in the internal arrangement of tissues (e.g., due to biochemical stress (Chiera et al., 2002) or water loss (Martin et al., 1991)) the three-dimensional geometrical description of the cells, which are represented by oblate ellipsoids, cylinders and spheres, has to change accordingly. The implementation of such geometrical changes is time consuming, and it may increase the operational costs of the model.

The ABM, which was developed primarily for computer graphics (visible light) applications, simulates the propagation of light within a plant leaf as a stochastic process whose states are represented by the main foliar tissue interfaces. We remark that while other stochastic models (Maier et al., 1999; Tucker & Garratt, 1977) iteratively simulate the chain of events (light interactions) occurring in the leaf tissues by explicitly forming and multiplying transition (probability) matrices, the ABM traces the light (ray) interactions by computing their probabilities on the fly.

The ABM accuracy is also dependent on availability of reliable input data. The simulation of changes in the internal arrangement of the tissues can be performed with a smaller operational overhead using this level of abstraction, however, since it does not involve the modeling and positioning of geometrical primitives (e.g. cylinders, spheres and ellipsoids).

Selecting the "best" model for a given application is a delicate task, and no single modeling approach is superior in all instances. This task may require an analysis of the application requirements (e.g., accuracy and predictability) and constraints (e.g., data availability and computational costs). In some cases, the development of practical simulation solutions may demand the implementation of a variety of models, with the one actually employed chosen at runtime dependent on the foliage's characteristics. Alternatively, different models can be combined to provide hybrid solutions. For example, Bousquet et al. (2005) proposed an approach aiming at inversion procedures which consists in combining a BRDF model with a spectral reflectance and transmittance model for plant leaves, PROSPECT (Jacquemoud & Baret, 1990), to fit BRDF measurements.

Clearly, the predictive and accurate modeling of radiation propagation and absorption in plant leaves is still an open problem in remote sensing and related fields such as experimental botany. In this paper, we present alternative simulation strategies for the investigation of these phenomena. They consists in two models, ABM-B and ABM-U, which are used to simulate the interaction of radiation with bifacial and unifacial plant leaves, respectively. Although their design is based on a Monte Carlo approach similar to the one used in the ABM, they take into account a larger number of foliar optical interfaces, and their formulation incorporates features that are essential for the accurate and predictive simulation of radiation transport and absorption in plant leaves as well as the effects of foliar structural changes on these processes. These aspects, namely accuracy and predictability, were favourably evaluated through comparisons of modeled results with actual measured data. We remark that the ABM was primarily aimed at the visible region of the light spectrum, and considered only four interfaces, namely air ⇔ adaxial epidermis, mesophyll ⇔ air, air ⇔ abaxial epidermis and abaxial epidermis ⇔ air.

There is an increasing demand for simulation tools to assist investigations involving foliar optical properties in the infrared domain. Such investigations are crucial to the assessment of the biochemistry and water stress of regions of vegetation (Wessmann, 1990), and to the improvement of the current understanding of the physiological phenomena that relate plant leaf spectral signatures to foliar compounds interacting with electromagnetic radiation (Fourty et al., 1996; Jacquemoud et al., 1996). For these reasons, the examination of the proposed models focuses on theoretical and practical issues associated with infrared applications.

2. Algorithmic models

In this section, we describe the proposed algorithmic models, ABM-B and ABM-U, and highlight the aspects that represent major changes with respect to the ABM. For detailed information on simulation techniques previously applied in the ABM, the reader is referred to the texts by Baranoski and Rokne (1997, 2004). Both proposed models apply geometrical or ray optics concepts, and associate the wavelength of incident radiation, a physical optics parameter, to each sample ray.

2.1. ABM-B

Although plant leaves have been concisely described by Woolley (1971) as a pigmented structure, mesophyll, having external plates of epidermal cells with a protective extracellular membrane, called cuticle, they are in fact complex optical systems. The cuticle is composed mostly of cutin and soluble lipid substances deposited on the surface as epicuticular wax (Holloway, 1982). The surface roughness characteristics and the refraction index of the epicuticular wax control the specularly reflected light from the front (adaxial) and back (abaxial) epidermis. No intercellular spaces are normally present in the epidermal tissues.

Bifacial leaves are characterized by a differentiated mesophyll which is usually composed of one or more layers of palisade cells with a cylindrical shape, and a loosely packed

layer of spongy cells roughly ovoid to round in shape. The palisade tissue may have 5% to 20% of its volume occupied by air space, whereas the spongy tissue may have 50% to 80% of its volume occupied by air space (Woolley, 1971).

In the ABM-B, radiation propagation is simulated as a random walk process whose states correspond to the main tissue interfaces found in bifacial leaves. Fig. 1 presents the interfaces considered in the ABM-B formulation. The transition probabilities of this random walk are associated with the Fresnel coefficients computed at each interface, and the termination probabilities are associated with the free path length of the ray traveling in the mesophyll tissue.

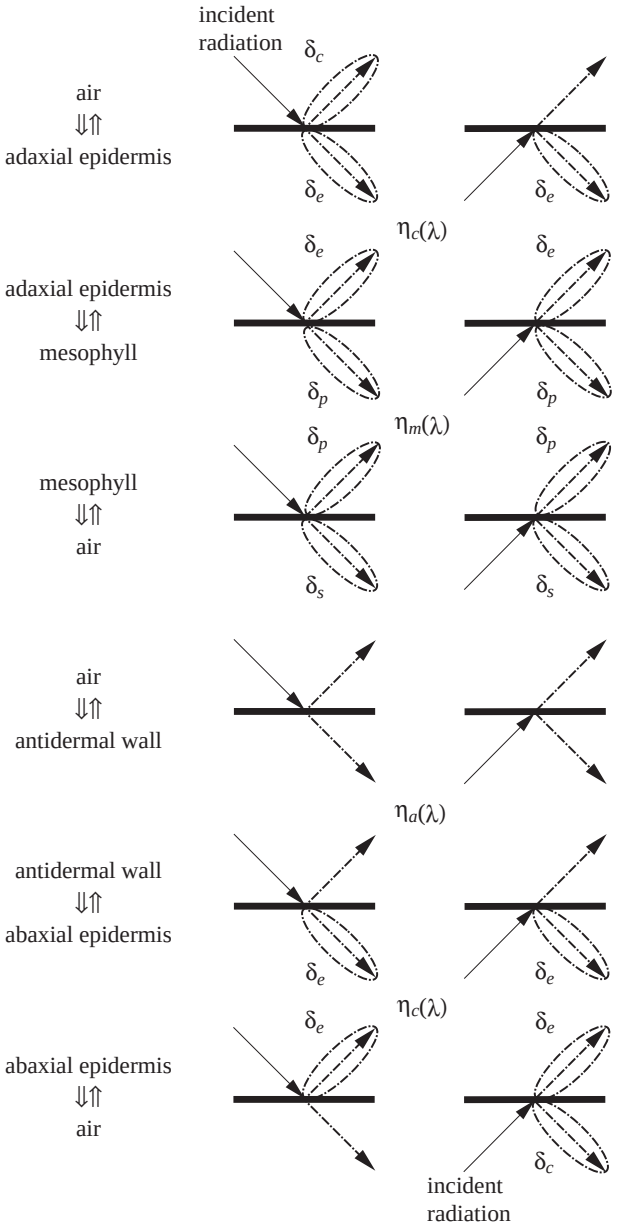

Fig. 1. Perturbations performed by the ABM-B on the propagated rays at each interface considered in the representation of bifacial leaves. The parameters δ_c, δ_e, δ_p and δ_s correspond to the aspect ratio of the cuticle undulations, epidermis cell caps, mesophyll palisade cell caps and mesophyll spongy cell caps, respectively. The parameters $\eta_c(\lambda)$, $\eta_m(\lambda)$ and $\eta_a(\lambda)$ correspond to the spectral refractive index of the cutinized epidermal cell wall, the mean spectral refractive index of the wet mesophyll cell wall and the mean spectral refractive index of the antidermal cell wall, respectively.

The computation of Fresnel coefficients requires as input the angle of incidence of the incoming ray as well as the refractive indices of the incidence and transmissive media. Since the materials present in hydrated (wet) tissues form an aqueous solution, we use for these tissues the mean spectral refractive index (Tuchin, 2000) which is given by:

$$\eta(\lambda) = c_s\eta_s(\lambda) + (1 - c_s)\eta_b(\lambda) \quad (1)$$

where:

c_s volume fraction of scatterers,
η_s refractive index of the scattering material,
η_b refractive index of the base material.

The scattering material corresponds to the actual scatterers, and the base material corresponds to ground matter or the medium in which these scatterers are dispersed (Tuchin, 2000). Usually the refractive indices available in the literature for the scattering materials correspond to either values averaged across the entire electromagnetic spectrum, or values measured at an specific wavelength. Despite this practical constraint, we believe that it is worthwhile to make an effort to use spectral refractive indices whenever they are available.

In our simulation of bifacial leaves, the mean spectral refractive index of the wet mesophyll cell wall, $\eta_m(\lambda)$, is computed using the refractive index of the dry mesophyll cell wall as the refractive index for the scattering (dry) material, and the refractive index of water, $\eta_w(\lambda)$, as the refractive index for the base material. Similarly, the mean spectral refractive indices of the wet antidermal cell wall (abaxial epidermis cell wall in contact with the internal tissues (Woolley, 1975)), $\eta_a(\lambda)$, is computed using the refractive index of the dry antidermal cell wall as the refractive index for the scattering (dry) material.

The refractive index of the cutinized epidermal cell wall, $\eta_c(\lambda)$, used in our simulations corresponds to the refractive index of the epicuticular wax. This choice is based on observations that the greatest discontinuity between refractive indices for foliar tissues is across the air-wax boundary (Vanderbilt, 1985; Vanderbilt et al., 1991).

After computing the Fresnel coefficient (F) at an interface, we compared it with a random number ξ_f computed on the fly. If $\xi_f \leq F$, then we generate a reflected ray, otherwise we generate a transmitted ray. The reflected ray is computed applying the law of reflection, and the transmitted ray is computed applying Snell's law.

Brakke et al. (1989) noted that an exponentiated cosine function could provide a good approximation for the scattering profile of foliar tissues which, in the context of this paper, refers to the spatial power distribution of the propagated radiation. The ABM-B uses a similar approach to simulate the distribution of the rays reflected or transmitted at the foliar interfaces. These rays are perturbed using a warping function (Eq. (2)). This function corresponds to a probability distribution function (PDF) based on an exponentiated cosine distribution, where the exponent is given by the aspect ratio

of the cell regions interacting with radiation, henceforth referred to as cell caps. The perturbation is performed through angular displacements, α and β. The angle α corresponds to the polar angle with respect to the ideal reflection or ideal transmission direction. The angle β corresponds to the azimuthal angle around the ideal reflection or ideal transmission direction. These angles are given by:

$$(\alpha,\beta)=\left(\arccos\left(\left(1-\xi_{\mathrm{p}}\right)^{\frac{1}{\delta+1}}\right),2\pi\xi_{\mathrm{a}}\right) \tag{2}$$

where:

ξ_{p} uniformly distributed random number $\in[0,1]$,
ξ_{a} uniformly distributed random number $\in[0,1]$,
δ aspect ratio of the cell cap.

In the models described in this paper, the aspect ratio of a cell cap is defined as:

$$\delta=w/h \tag{3}$$

where:

w cell cap width,
h cell cap height.

The cell cap width and height correspond to average values measured in the planes parallel and perpendicular to the foliar plane, respectively. Foliar tissues whose cells have an oblate shape (large δ) have a scattering profile closer to a specular distribution than tissues whose cells have a round shape (small δ).

It is important to note that the energy conservation properties of a PDF based on an exponentiated cosine function become less physical as the exponent approaches zero, and the resulting behavior tends to become that of a mirror when the exponent approaches infinity. By associating the exponent of the warping function with a biological meaningful parameter, the range for this parameter becomes bound by predictable values, which prevents a violation of the energy conservation properties. The lower bound value (1.0) used in our simulations corresponds to a cosine (diffuse) distribution. This value for δ may be used to simulate the scattering profile of specimens whose mesophyll is characterized by the presence of a densely packed layer of palisade cells heavily populated by chloroplasts. The upper bound values for δ used in our simulations (Tables 4 and 5) are derived from cell dimensions found in the literature as described in Section 3.

Fig. 1 presents the perturbations performed at each interface in both directions, upwards and downwards. In order to be consistent with available biological information and to avoid undue complexity, a conservative strategy was adopted. It consists in warping the rays only where this perturbation has a noticeable effect on the overall BDF.

Once a ray enters the mesophyll tissue, it may be propagated or absorbed. The absorption testing performed by the ABM-B is based on the expression used by Allen et al. (1969) to compute the transmissivity of a medium according to a variation of Beer's law. The stochastic interpretation of this expression indicates that the probability of absorption of a photon (ray) traveling a distance Δp at a certain wavelength λ in the medium is given by:

$$P(\lambda)=1-e^{-\mu_a(\lambda)\Delta p\,\sec(\theta)} \tag{4}$$

where:

$\mu_{\mathrm{a}}(\lambda)$ effective absorption coefficient of the medium (1/cm),
θ angle between the ray direction and the medium's normal direction.

The effective absorption coefficient is obtained by adding the absorption coefficients of the medium's constituent materials, which, in turn, are obtained by multiplying the specific absorption coefficient (s.a.c.) of each material (given in $\mathrm{cm}^2/\mu\mathrm{g}$) by its concentration in the medium (given in $\mu\mathrm{g}/\mathrm{cm}^3$). The absorption coefficient of water corresponds simply to its s.a.c. (given in 1/cm).

By inverting Eq. (4), the following expression used to estimate the free path length of a slant ray traveling in the mesophyll tissue is obtained:

$$p(\lambda)=-\frac{1}{\mu_{\mathrm{a}}(\lambda)}\ln(\xi_{\mathrm{r}})\cos(\theta) \tag{5}$$

where:

ξ_r uniformly distributed random number $\in[0,1]$.

If $p(\lambda)$ is greater than the thickness of the medium, t_{mb}, the ray is propagated, otherwise it is absorbed. The thickness value used as input for ABM-B corresponds to a fraction of the total thickness of a bifacial leaf, t_{b}. Based on the morphological characteristics of bifacial leaves (Bowes, 1996; Chiera et al., 2002; Woolley, 1971, 1973), we estimate that t_{mb} usually corresponds to approximately 50% of t_{b} for fully developed and healthy specimens.

2.2. ABM-U

Unifacial leaves are characterized by an undifferentiated mesophyll, which is usually composed of cells roughly ovoid to round in shape, attached to both the front and the back epidermal layers (Bowes, 1996). In monocotyledon species with unifacial leaves, this tissue visually resembles the spongy mesophyll of bifacial leaves, but with a smaller portion of its volume occupied by air, as illustrated in cross-section photographs of unifacial and bifacial leaves available in the literature (Breece & Holmes, 1971; Vogelmann & Martin, 1993).

In the ABM-U, radiation propagation is also simulated as a random walk process whose states correspond to the main tissue interfaces found in unifacial leaves. Fig. 2 presents the interfaces considered in the ABM-U formulation. Similarly to the ABM-B, the ABM-U determines the reflection and transmission of rays incident on each interface by computing the corresponding Fresnel coefficients, and perturbing the

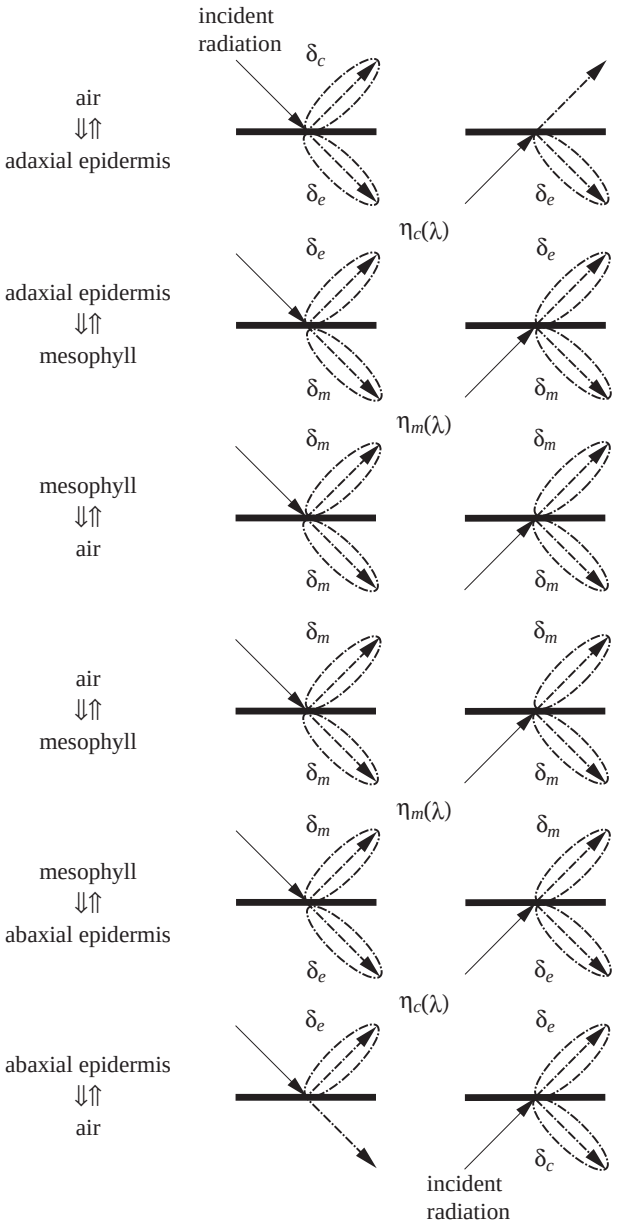

Fig. 2. Perturbations performed by the ABM-U on the propagated rays at each interface considered in the representation of unifacial leaves. The parameters δ_c, δ_e, δ_m correspond to the aspect ratio of the cuticle undulations, epidermis cell caps and mesophyll cell caps, respectively. The parameters $\eta_c(\lambda)$ and $\eta_m(\lambda)$ correspond to the spectral refractive index of the cutinized epidermal cell wall and the mean spectral refractive index of the wet mesophyll cell wall, respectively.

propagated rays. The computation of Fresnel coefficients takes into account the mean refractive index of wet tissues (Eq. (1)) and the refractive index of the cutinized epidermal wall. The perturbation of propagated rays is also performed using the warping function based on an exponentiated cosine function (Eq. (2)).

Although the absorption of a propagated ray is also determined probabilistically by computing its free path length (Eq. (5)), it takes into account the morphology of the unifacial leaves' mesophyll. While in bifacial leaves larger air spaces are found in the spongy mesophyll layer, in unifacial leaves the air spaces are more uniformly distributed throughout the whole thickness of the mesophyll tissue, t_{mu}. Hence, for each ray incident on an unifacial leaf, we generate a random number ϱ uniformly distributed in the interval [0,1], which we multiply by t_{mu} to probabilistically determine the location of an internal air space. If the ray travels in the portion of the leaf above this internal air space (Fig. 2), then we compare the $p(\lambda)$ with ϱt_{mu}, otherwise we compare it with $(1-\varrho)\, t_{mu}$. If $p(\lambda)$ is greater than the adjusted t_{mu}, then the ray is propagated, otherwise it is absorbed. Based on the morphological characteristics of unifacial leaves (Bowes, 1996; Vogelmann & Martin, 1993), we estimate that t_{mu} usually corresponds to approximately 80% of their total thickness, t_u, for fully developed and healthy specimens.

3. Data and evaluation issues

We selected, without loss of generality, species representative of bifacial and unifacial leaves, namely soybean (*Soja hispida* or *Glycine max L.*) and maize (*Zea mays L.*), respectively, to be used in our evaluation of the proposed models. We remark that these two species are also representative of dicotyledons and monocotyledons plants, respectively. This choice was motivated by two aspects. First, these species are of direct interest in remote sensing since they represent agriculturally valuable crops (Breece & Holmes, 1971). Second, due their economical importance, structural and biophysical data for soybean and maize, popularly known as corn, are more readily available in the scientific literature than for species less economically important. This aspect is relevant since a well designed model is of little use without reliable specimen characterization data to be used as input and accurate optical data against which it can be evaluated.

In order to evaluate the accuracy and predictability of the proposed models, we have compared modeled results to measured data available in the Leaf Optical Properties Experiment (LOPEX) database (Hosgood et al., 1995) as well as measured data published in the literature (Breece & Holmes, 1971; Woolley, 1971). For the comparisons involving measured soybean reflectance and transmittance curves we used LOPEX spectral files 0219 and 0220, respectively, while for the comparisons involving measured corn reflectance and transmittance curves we used LOPEX spectral files 0141 and 0142, respectively. These comparisons were performed using a virtual spectrophotometer (Baranoski et al., 2001) and a virtual goniophotometer (Krishnaswamy et al., 2004).

Ideally, all foliar tissue constituent materials that affect the transport and absorption of radiation by plant leaves should be incorporated in the evaluation experiments. However, data for several of such materials is not available in the literature. The data is even more scarce for materials in their pure form, and usually their absorption profile is only implicitly indicated in terms of reflectance or absorptance spectra (Barton et al., 1990; Davies & Grant, 1988; Verdebout et al., 1994; Wessmann, 1990; Weyer, 1985), i.e., their specific absorption coefficients (s.a.c.) are not provided. For these reasons, in our experiments, we have considered only the main foliar constituent materials

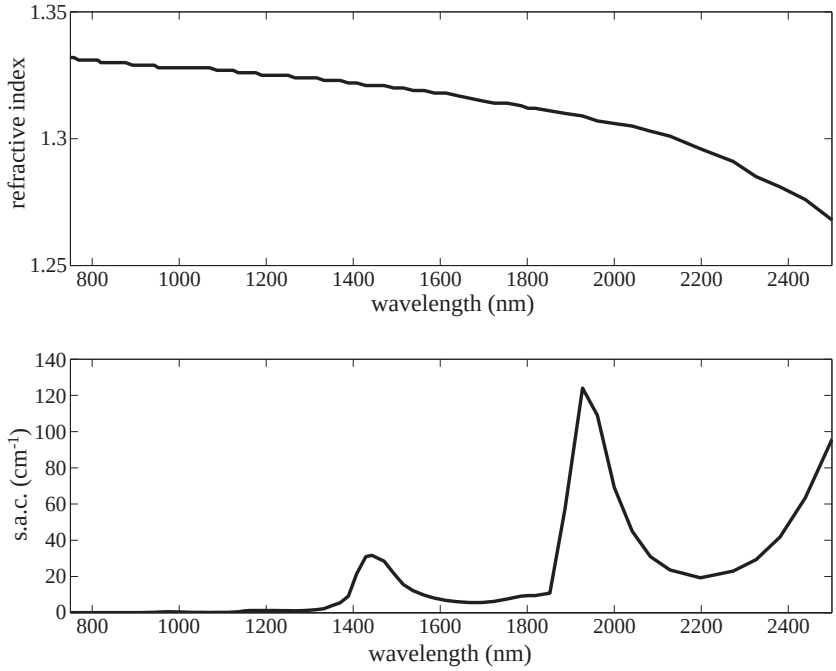

Fig. 3. Refractive index and specific absorption coefficient (s.a.c.) for water at 27 °C (Palmer & Williams, 1974).

interacting with infrared radiation: protein, cellulose+lignin and water. The refractive index and s.a.c. curves for water used in our experiments (Fig. 3) were published by Palmer and Williams (1974). The s.a.c. curves for protein and cellulose+lignin used in our experiments (Fig. 4) were obtained from estimated data for fresh and dry leaves provided by Jacquemoud et al. (1996), and scaled according to a procedure indicated by Ganapol et al. (1999). The scaled s.a.c. curve for protein was previously applied by Johnson (2001) to study the nitrogen influence on fresh leaf near infrared spectra. As stated by Jacquemoud et al. (1996), there is a strong relationship between total nitrogen and protein content. Such relationship is taken into account in our experiments as well. It is worth noting that s.a.c. curves for the foliar constituents considered in these experiments as well as other constituents, such as starch and sugar, have been estimated by Fourty et al. (1996) for dry leaves. We choose to use data estimated for both fresh and dry leaves since, as stated by Jacquemoud et al. (1996), most of the time regions of vegetation are observable by airborne or remote sensing sensors in the fresh green state, thus, there is a need for

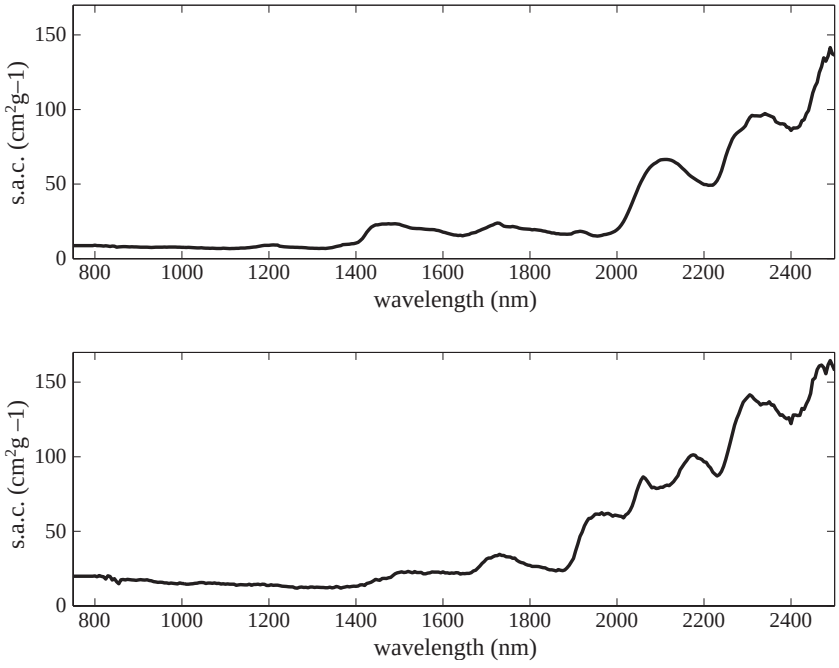

Fig. 4. Specific absorption coefficient (s.a.c.) for cellulose+lignin (top) and protein (bottom) obtained from estimated data provided by Jacquemoud et al. (1996), and scaled according to procedure indicated by Ganapol et al. (1999).

developing simulating strategies that are more sensitive to changes in fresh leaves.

An important factor affecting evaluation experiments is the input data, i.e., the data used to characterize the biophysical properties of the specimens whose measured curves of spectral power distribution (reflectance and transmittance) are being used in the comparisons. Clearly, one would like to use only data obtained directly from measurements on the specific specimens used in the experiments. Such data is usually only partially available, however. For example, although LOPEX provides biochemical characterization data, such as weight and thickness, for the specimens, the values for other optical and structural parameters, such as refractive indices, cell dimensions and air volumes, need to be derived from average values published in the literature.

Table 1 presents the LOPEX biophysical data for the soybean and corn specimens used in our experiments. The measurements of total protein (nitrogen), cellulose and lignin available in LOPEX were performed on 250 g of partially dried soybean and corn materials, i.e., they represent average values for each species instead of being specimen specific. These measurements were performed by two different laboratories, one in France and another in Belgium, which provide slightly different sample/biochemical data sets, henceforth referred to as data sets F and B, respectively. Table 2 presents the percentages of biochemical constituents for the species used in our experiments. The graphical results presented in this paper were obtained using data set B. Experiments performed using data set F yield similar results, and the small numerical differences observed using the two data sets are presented in the next section.

The concentrations of the tissue constituents considered in our experiments (Table 3) were obtained by multiplying the concentration of dry matter in each specimen by the percentages indicated in Table 2. The concentrations of dry matter, in turn, were computed by dividing the specimen's dry weight by its "nonair" volume, i.e., the total volume minus the air volume. The total volume is given by the product of the area of the samples used in the LOPEX measurements (4.10 cm^2) by the specimen's thickness (Table 1). The air volumes used in our experiments for the soybean and corn specimens were 31% and 12.7% of the total volume, respectively (Woolley, 1973).

In order to determine the parameter c_s used to compute the mean refractive indices of wet cell walls (Eq. (1)), we used the refractive index of the wet antidermal wall (1.41) and the refractive index of the dry antidermal wall (1.535), both measured at 800 nm (Woolley, 1975), and the refractive index of water (1.331) also measured at 800 nm (Palmer & Williams, 1974). Placing these values in Eq. (1) yields $c_s=0.3872$. Using this value, and replacing η_s by 1.535 in Eq. (1), we obtain the approximative expression for the mean spectral refractive index of the wet antidermal wall used in our experiments:

$$\eta_a(\lambda) = 0.5943 + \eta_w(\lambda)0.6128 \quad (6)$$

Considering the biochemical similarities between the antidermal and mesophyll walls and the scarcity of data for the latter, we use the same volume fraction of scatterers for both walls in our experiments. Thus, the refractive index of the dry mesophyll cell wall at 800 nm is obtained using $c_s=0.3872$, the refractive index of wet mesophyll cell wall (1.42) measured at 800 nm (Woolley, 1975) and the refractive index of water (1.331) also measured at 800 nm (Palmer & Williams, 1974). Plugging these values in Eq. (1), yields an estimated refractive index of 1.5608 for the dry mesophyll cell wall. Replacing η_s in Eq. (1) by this value, and using $c_s=0.3872$, we obtain the approximative expression for the mean spectral refractive index of the wet mesophyll wall used in our experiments:

$$\eta_m(\lambda) = 0.6043 + \eta_w(\lambda)0.6128 \quad (7)$$

The refractive indices for cell walls mentioned above were measured by Woolley (1975) using soybean leaves. To the best of our knowledge, values for corn leaves are not available in the literature, except for a whole leaf (Allen et al., 1969). For this reason, we use the same approximating expression for the mean refractive index of the wet mesophyll cell wall in the soybean and corn experiments.

Although it is possible to find the refractive indices for few plant waxes in the literature (Allen et al., 1969; Weast, 1989) and other substances present in the cutinized epidermal cell wall (e.g., cutin has a reported refractive index of about 1.5 (Holloway, 1982)), their wavelength dependence is usually omitted. Since the research presented in this paper is aimed at infrared applications, we choose to use in our experiments the wavelength dependent refractive indices for epicuticular wax estimated by Vanderbilt (1985) for the interval between 750 and 1000 nm. Due to the lack of information regarding their wavelength dependence beyond 1000 nm, we used for this region the value estimated at 1000 nm (1.478) by Vanderbilt

Table 2
Species specific data provided by LOPEX

Constituents	Data set F		Data set B	
	Soybean	Corn	Soybean	Corn
Protein	31.06%	25.31%	31.64%	26.55%
Cellulose	14.90%	21.80%	16.83%	26.60%
Lignin	4.24%	2.19%	2.90%	3.03%

Table 1
Specimen specific data provided by LOPEX

Biophysical data	Specimens	
	Soybean	Corn
Fresh weight	0.0494 g	0.0668 g
Dry weight	0.0119 g	0.0146 g
Thickness	0.0166 cm	0.0204 cm

Table 3
Concentrations of the tissue constituents derived from LOPEX sample/biochemical data sets B and F

Constituents	Data set B		Data set F	
	Soybean	Corn	Soybean	Corn
Protein	0.0801 g/cm^3	0.0530 g/cm^3	0.0787 g/cm^3	0.0506 g/cm^3
Cellulose+lignin	0.0499 g/cm^3	0.0592 g/cm^3	0.0485 g/cm^3	0.0479 g/cm^3

and Grant (1985). Also due to lack of specific data for each species, we use the same values for both specimens.

The cell cap aspect ratios used in our experiments (Tables 4 and 5) were derived from data available in the literature (Bone et al., 1985; Govaerts et al., 1996; Martin et al., 1991; Vogelmann & Martin, 1993), and also borne out by observations of cross-sections of soybean and corn leaves (Breece & Holmes, 1971). The aspect ratio of cuticle undulations should be adjusted according to its thickness and morphology. Although, to the best of our knowledge, quantitative information for soybean and corn leaves with respect to these structural cuticular characteristics is not available in the literature, their effect on the polarized surface reflectance have been examined by Grant et al. (1993). Based on the magnitude ratio of the polarized surface reflectances measured for soybean and corn specimens at 750 nm (Grant et al., 1993), approximately 1 : 2, and observations of cross-sections of soybean and corn leaves (Breece & Holmes, 1971), we have performed a proportional adjustment in the aspect ratio of the corn specimen's cuticle undulations in comparison with the value used for the soybean specimen.

The characteristics of the adaxial and abaxial cuticles of plant leaves usually differ. In order to represent such differences which qualitatively affect the BRDF of plant leaves (Brakke, 1994), one can adjust the aspect ratio of surface undulations found in the adaxial and abaxial cuticles. Due to lack of measured structural data for these surfaces, such adjustment might be also guided by the measured polarized reflectance of these surfaces. For example, the polarized reflectance of a soybean leaf measured at 750 nm from the abaxial surface (Grant et al., 1993) corresponds to approximately half the value measured from the adaxial surface. In this case, the parameter δ_c for the abaxial surface undulations would be reduced by a factor of two. For a corn leaf, the polarized reflectance value measured at 750 nm from the abaxial surface (Grant et al., 1993) corresponds to approximately twice the value measured from the adaxial surface. In this case, the parameter δ_c for the abaxial surface undulations would be increased by a factor of two.

Corn leaves present a reflectance behavior closer to a specular reflector when their veins are parallel to the measurement plane (Breece & Holmes, 1971; Woolley, 1971). The aspect ratio of the cuticle undulations may also be adjusted to mimic this asymmetric reflectance behavior, i.e., when the undulations are parallel to the measurement plane, the parameter δ_c may be increased to account for a reduction on the roughness of these undulations, which, in turn, increases the overall specularity of the corn leaf. The factor by which the aspect ratio may be adjusted also depends on the availability of measured structural data for the surface undulations, however. It is worth mentioning that this anisotropic behavior is more noticeable when the BRDF is measured at wavelengths that correspond to low absolute reflectance values. In this cases, the relative contribution of the near Lambertian subsurface reflectance component to the overall BRDF is reduced, and the contribution of the directional surface reflectance component can be observed.

Table 4
Aspect ratios selected for the bifacial (soybean) specimen

δ_c	δ_e	δ_p	δ_s
5.0	5.0	1.0	5.0

Table 5
Aspect ratios selected for the unifacial (corn) specimen

δ_c	δ_e	δ_m
10.0	5.0	5.0

In order to avoid the introduction of undue complexity and bias in our BRDF comparisons with measured data, we assume that the corn leaf's veins are perpendicular to the measurement plane in our experiments. It is worth noting that our BDF experiments were performed at 1000 nm to allow a qualitative comparison with infrared BRDF and BTDF values published in the literature (Breece & Holmes, 1971), and the absolute reflectance and transmittance values for wavelengths in the near infrared region are fairly high, i.e., the corn leaf's anisotropic behavior mentioned above becomes negligible.

4. Results and discussion

Figs. 5 and 6 present comparisons between modeled and measured reflectance and transmittance curves for the soybean and the corn specimens, respectively. The measured curves are available in the LOPEX database, and they correspond to an angle of incidence of 8°. The same angle of incidence was used to obtain the modeled curves. As can be observed in these graphs, the quantitative differences between the modeled and measured curves are relatively small for most of the wavelengths being considered. It is important to note, however, that for regions where the spectral curves have steep slopes, the differences may be greater than it is indicated by the visual proximity between the modeled and experimental curves. For this reason, we have also computed the root mean square errors (RMSE) for these curves. The RMSE values are given in Table 6 and correspond to experiments considering the biochemical/sample information provided in the data sets B and F. All reported RMSE values are smaller than 0.03, which, according to Jacquemoud et al. (1996), indicates good spectrum reconstruction for both bifacial and unifacial leaves, and for both reflectance and transmittance curves.

The comparisons presented in Figs. 5 and 6 also indicate that there is still room for quantitative improvement. It is important to note, however, that despite our data gathering efforts, the characterization data sets available for each specimen are somewhat limited. For example, refractive indices and structural characteristics, such as air volume and cell dimensions, needed to be derived from average values available in the literature, and these values may not correspond exactly to the characteristics of the foliar specimens used in the LOPEX measurements. Furthermore, spectral data, such as the absorption spectra of biochemical constituents, correspond to estimated values, instead of data measured for pure substances. Clearly, such data limitations affect the accuracy of modeled curves, and quantitative improvements on the modeling of foliar optical properties will likely require major multidisciplinary measurement efforts.

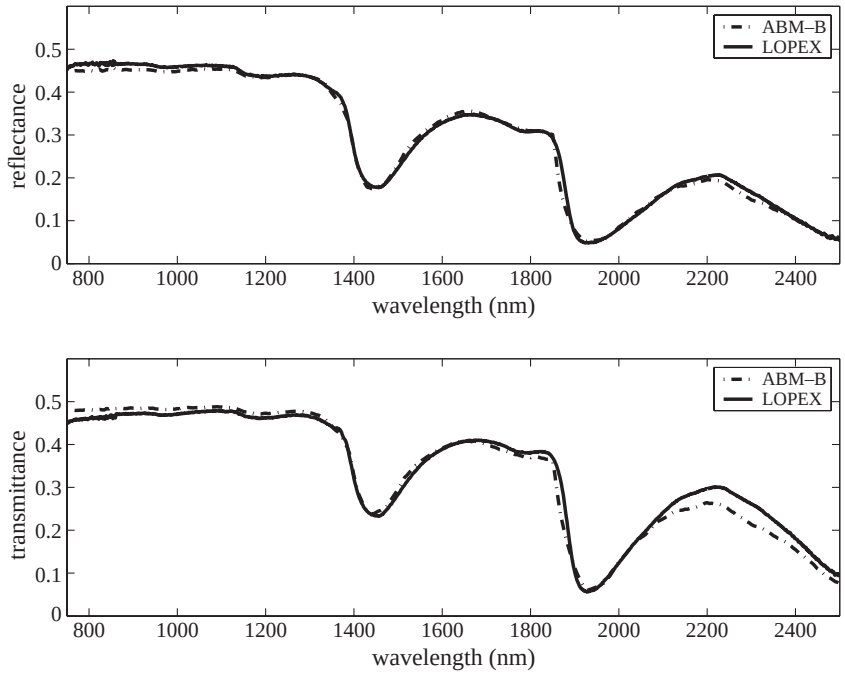

Fig. 5. Measured (LOPEX) and modeled (ABM-B) spectral curves for a fresh soybean leaf considering an angle of incidence of 8°.

Besides the quantitative comparisons described above, we also performed qualitative comparisons against actual observations of real phenomena to demonstrate the predictability of the proposed models. In these comparisons, we take into account data measured by Woolley (1971) for soybean and corn specimens which consider an angle of incidence of 2.5°. In order to be consistent with the actual observations, we use the same angle of incidence in our experiments whose results are shown in Figs. 7 and 8.

Observations by Woolley (1971) indicate that bifacial leaves show greater reflectance for their abaxial epidermis (back) than for their adaxial epidermis (face), except for near infrared domain from 750 to 1300 nm, where the faces have higher reflectance. Furthermore, these leaves show greater transmittance over the entire infrared domain when their backs are toward the light source, and less transmittance when their faces are toward the light source. Fig. 7 demonstrates that the ABM-B can predict these phenomena for bifacial leaves. Furthermore, it is important to note that the modeled curves show a striking qualitative agreement with the curves measured by Woolley (1971) to investigate these phenomena for soybean leaves.

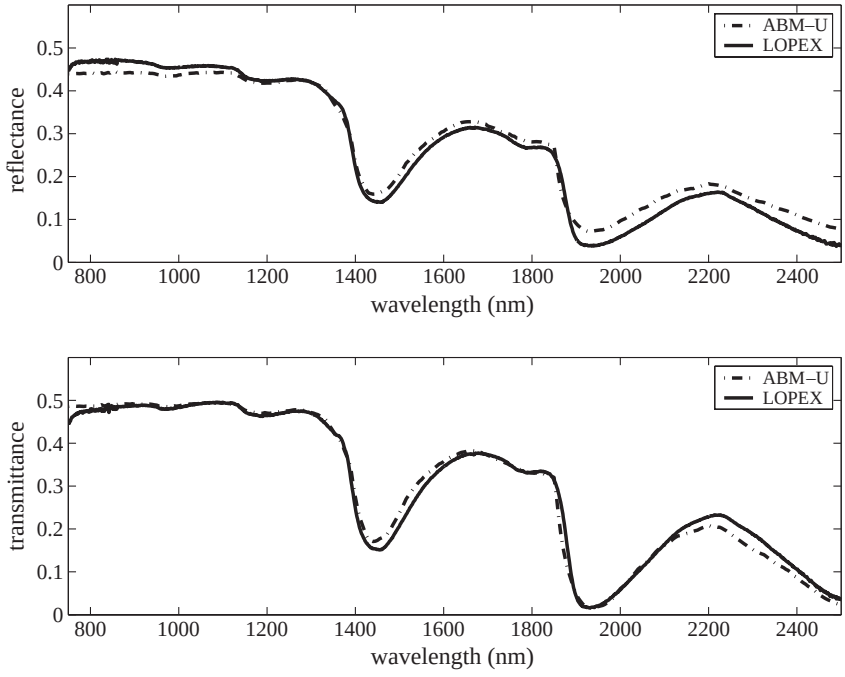

Fig. 6. Measured (LOPEX) and modeled (ABM-U) spectral curves for a fresh corn leaf considering an angle of incidence of 8°.

Table 6
RMSE values of measured vs. modeled spectral curves obtained using LOPEX sample/biochemical data sets B and F

Species	Data set B		Data set B	
	Reflectance	Transmittance	Reflectance	Transmittance
Soybean	0.0114	0.0208	0.0111	0.0206
Corn	0.0231	0.0178	0.0238	0.0174

Due to the relatively symmetrical structure of an unifacial leaf, one may expect symmetry in the spectral power distribution (reflectance and transmittance) for top and bottom incidence (Breece & Holmes, 1971). The correct simulation of this symmetric behavior is guaranteed by the ABM-U symmetrical design.

Experiments by Woolley (1971) demonstrate that the reflectance of an unifacial leaf is not strongly dependent on the leaf thickness, within usual ranges, except for near infrared domain from 750 to 1300 nm, where a thick unifacial leaf shows greater reflectance than a thin leaf. This behavior was also observed in laboratory reflectance measurements performed by Maracci et al. (1991) on water stressed corn leaves. The transmittances, however, are more strongly influenced by the thickness of an unifacial leaf, with a thin unifacial leaf showing greater transmittance over the entire infrared domain. According to Woolley (1971), the cause of these observed differences may be due to changes in internal arrangement of the tissues. These changes are related to the fact that unifacial leaves, such as corn leaves, shrank mostly in thickness. Thus, a reduction of their thickness, e.g., due to loss of water (Woolley, 1975), without accompanying lateral shrinkage, can cause flattening of the mesophyll cells, which, in turn, may cause changes in the internal scattering profile of these leaves. In order to evaluate the ABM-U predictive capabilities, we performed experiments in which we consider a 20% reduction of the corn specimen's thickness accompanied by a 20% increase in the aspect ratio of its mesophyll cell caps. The results presented in Fig. 8 demonstrate that the ABM-U can predict these phenomena for unifacial leaves. Again, it is important to note that the modeled curves show a striking qualitative agreement with the curves measured by Woolley (1971) to investigate these phenomena for corn leaves.

The role of foliar BRDF and BDTF in remote sensing investigations involving regions of vegetation is still object of discussion (Brakke, 1994; Chelle, 2003; Jacquemoud & Ustin, 2001). Nonetheless, such information can provide valuable insights with respect to the correctness of the scattering simulations performed by the model. For this reason, we have also performed experiments to qualitative evaluate the BRDFs (f_r) and BTDFs (f_t) provided by the proposed models. In order to facilitate the comparison with BRDF and BRDF curves measured in the infrared domain provided in the literature (Breece & Holmes, 1971), our polar BRDF and BTDF plots correspond to fractional curves, i.e., $f_r \cos \Theta_c$ and $f_t \cos (\pi - \Theta_c)$, respectively, where Θ_c corresponds to the collector angle.

A comprehensive evaluation of the scattering behavior predicted by proposed models would require the consideration of all possible illumination and viewing geometries as well as a fine spectral resolution. However, the large number of measurements needed as well as the lack of data covering all measuring instances preclude such thorough evaluation. For these reasons and for the sake of consistency with actual measurement conditions, our BDF experiments are performed with respect to the near infrared domain, with the BDF samples taken in the plane given by the direction of the incident radiation and the specimen's normal. This spectral and sample domains corre-

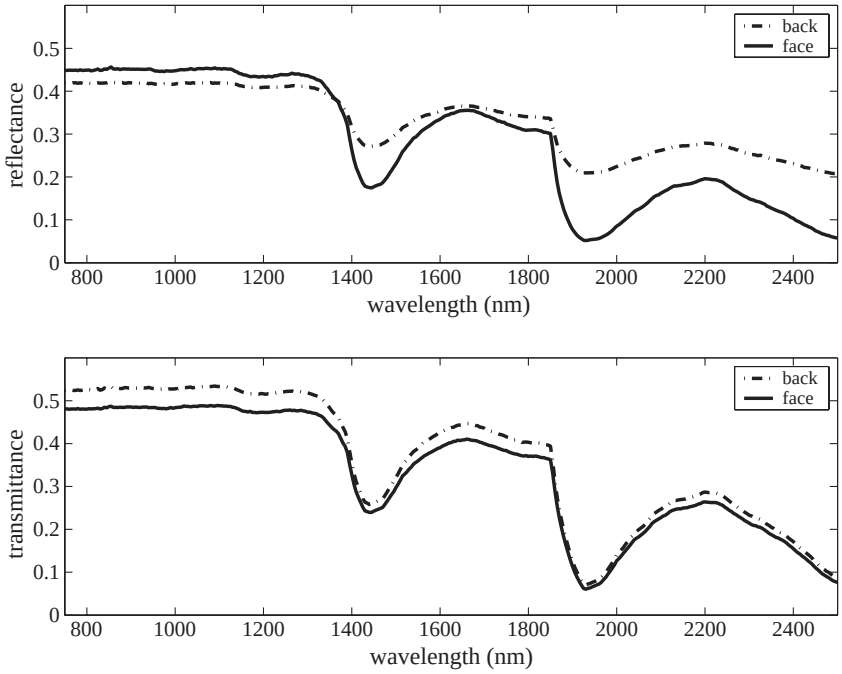

Fig. 7. Modeled (ABM-B) spectral curves for a soybean leaf considering its face (adaxial layer) and its back (abaxial layer) towards the light source which is positioned at an angle of incidence of 2.5°.

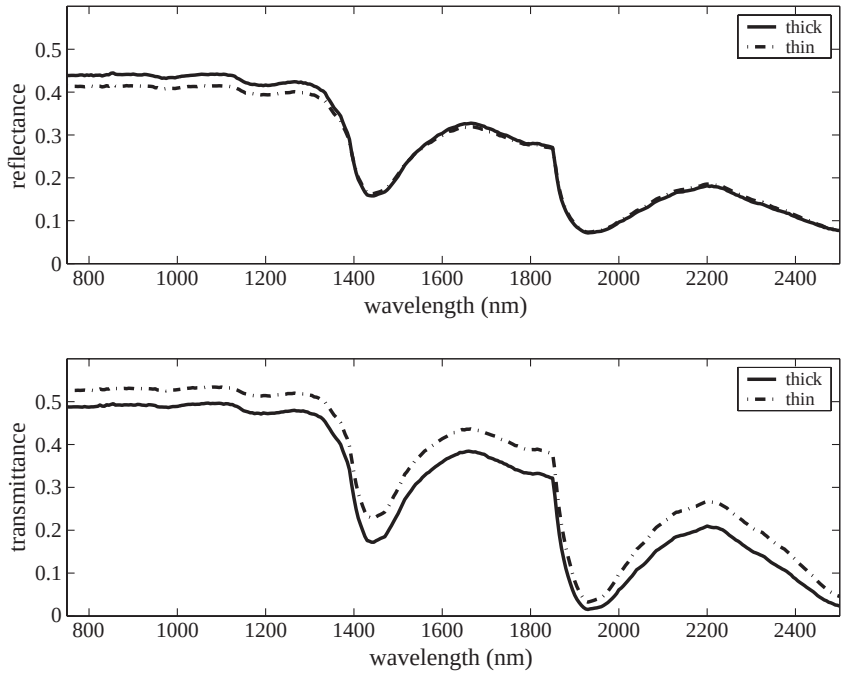

Fig. 8. Modeled (ABM-U) spectral curves for a corn leaf considering thickness variations: 204 μm (thick) and 163.2 μm (thin). The light source is positioned at an angle of incidence of 2.5°.

spond to the domains in which the actual BDF curves cited in our discussion (Breece & Holmes, 1971) have been measured.

Goniophotomteric (BRDF and BTDF) measured curves provided by Breece and Holmes (1971) show that, for wavelengths in the near infrared domain, soybean and corn leaves show a near Lambertian scattering behavior, and changes in the angle of incidence have a greater effect on the BRDF curves than on the BTDF curves. Such experimental observation is also confirmed by BRDF and BTDF experiments performed by Walter-Shea et al. (1989) on soybean and corn leaves. The modeled BRDF and BTDF plots presented in Figs. 9 and 10 indicate that the proposed models can simulate the scattering behavior observed in the actual measurements mentioned above. Furthermore, they generally agree with the BDF curves measured by Breece and Holmes (1971) which show a stronger directional behavior for the corn specimen's BRDF, and a near Lambertian behavior for the BTDF of both specimens.

For the near infrared wavelengths considered in the experiments by Breece and Holmes (1971), only a few percent of the incident radiation power are absorbed by the foliar tissues. Consequently, the near-Lambertian subsurface scattering component overwhelms the directional surface scattering component. Although the approach used by the proposed models to account for the spatial distribution of light reflected

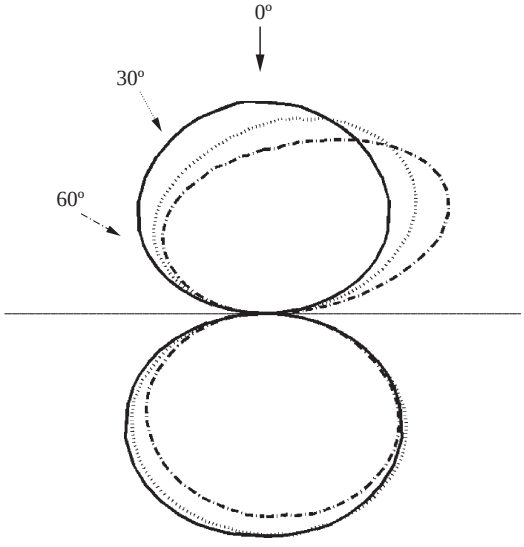

Fig. 9. Modeled (ABM-B) polar plots of a soybean leaf $f_r \cos \Theta_c$ and $f_t \cos (\pi - \Theta_c)$ computed at 1000 nm with respect to three angles of incidence: 0°, 30° and 60°.

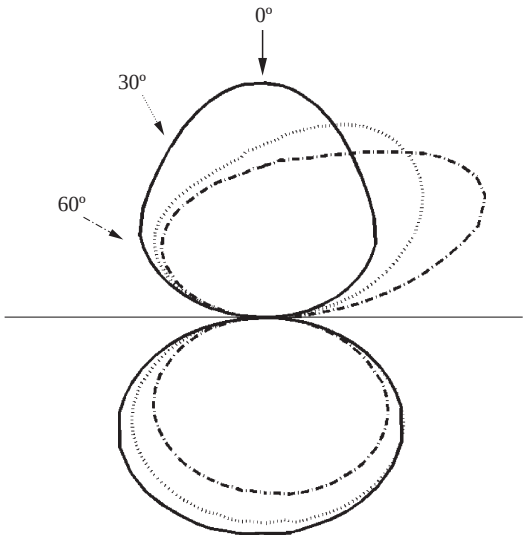

Fig. 10. Modeled (ABM-U) polar plots of a corn leaf $f_r \cos \Theta_c$ and $f_t \cos (\pi - \Theta_c)$ computed at 1000 nm with respect to three angles of incidence: 0°, 30° and 60°.

on the epicuticular layers approximates the actual surface scattering behavior, wave optics phenomena, such as polarization and diffraction, are not accounted for in the ray optics formulations used by ABM-B and ABM-U. More accurate representations of the surface scattering behavior of plant leaves will need to take into account the complex structure of the epicuticular waxes (Grant, 1987; Holloway, 1982), and to incorporate mathematical tools to account for these phenomena.

The proposed algorithmic models present a modular design. This aspect facilitates the replacement of the current procedures used to simulate the spatial power distribution of the radiation reflected on the epidermal surfaces by more robust ones as soon as they become available. Such replacement would not affect the accuracy and predictability of the proposed models with respect to spectral power distribution (reflectance and transmittance) of the incident radiation. There are, however, practical obstacles to the development of such routines, notably the lack of supporting measured data. Also, the inclusion of more complex algorithms to accurately model wave optics phenomena is likely to increase the computational costs of the simulations, with accuracy improvements noticeable only for spectral regions characterized by relatively high levels of absorption.

5. Conclusion

There is still a long way to go before the modeling of leaf optical properties can be considered a solved problem. Viewed in this context, the models proposed in this paper represent alternative simulation strategies for investigations involving foliar tissue optics. Their evaluation showed a general quantitative agreement between the modeled results and measured data. It is important to note, however, that quantitative evaluations may be affected by inherent difficulties to characterize testing specimens. Hence, we believed that, from a practical point of view, the predictive capabilities of the proposed models can provide a better assessment of their investigative usefulness. Promising evidence of such capabilities was provided by the qualitative agreement between the modeled results and observed phenomena. Furthermore, these qualitative tests demonstrated that the proposed models can take into account biophysical changes in the foliar tissues without incurring in a significant operational overhead.

Clearly, the modeling of the radiation transport and absorption by foliar tissues has a key role in the assessment of theories and data with respect to leaf optical properties, and the strength of the current understanding of such properties is essential to improve the benefits/costs ratio of remote sensing applications involving vegetation. However, as in any effort in physical sciences, models can become useful investigation tools only if evidence of their accuracy and predictability can be presented. As mentioned earlier, however, the evaluation of computer models of radiation interaction with plant leaves is bound by data availability. Although foliar reflectance and transmittance curves can be found in the scientific literature, they are usually restricted to a narrow range of measurement conditions. Moreover, high fidelity comparisons of modeled and measured quantities require reliable characterization data for the specimen at hand. Usually only averaged data is available for specimens used in foliar tissue optics experiments. In terms of goniophotometric (BRDF and BTDF) curves, despite valuable efforts of remote sensing researchers, there is still a shortage of data, and usually the available data sets present the same limitations outlined above for the reflectance and transmittance data sets. The lack of measured data is even more serious with respect to subsurface scattering data which, to the best of our knowledge, is available only for few species. Therefore, we believe that future improvements on the modeling of leaf optical properties will likely require not only researchers to bring more mathematical tools to bear on the problem, but also to direct substantial efforts towards the reliable measurement of multispectral surface and subsurface foliar data.

Acknowledgments

The author would like to thank the anonymous reviewers for their helpful suggestions. He is also grateful to the Joint Research Centre of the European Commission for granting him access to LOPEX data set which was established during an experiment conducted by the Advanced Techniques Unit of the Space Applications Institute (Italy). The work presented in this paper was supported by the Natural Sciences and Engineering Research Council of Canada (NSERC grant 238337) and the Canada Foundation for Innovation (CFI grant 33418).

References

Allen, W., Gausman, H., Richardson, A., & Thomas, J. (1969). Interaction of isotropic light with a compact plant leaf. *Journal of the Optical Society of America*, *59*(10), 1376–1379.

Arnold, L., Gillet, S., Lardiere, O., Riaud, P., & Schneider, J. (2002). A test for the search for life on extrasolar planets. *Astronomy and Astrophysics*, *392*, 231–237.

Baranoski, G. V. G., & Rokne, J. G. (1997). An algorithmic reflectance and transmittance model for plant. *Computer Graphics Forum*, *16*(3), 141–150.

Baranoski, G., & Rokne, J. (2004). *Light interaction with plants: A computer graphics perspective*. Chichester, Great Britain: Horwood Publishing.

Baranoski, G., Rokne, J., & Xu, G. (2001). Virtual spectrophotometric measurements for biologically and physically-based rendering. *The Visual Computer*, *17*(8), 506–518.

Barton, F., Himmelsbach, D., Duckworth, J., & Smith, J. (1990). Two-dimensional vibration spectroscopy: Correlation of mid and near-infrared regions. *Applied Spectroscopy*, *46*(3), 420–429.

Bone, R., Lee, D., & Norman, J. (1985, May). Epidermal cells functioning as lenses in leaves of tropical rain-forest shade plants. *Applied Optics*, *24*(10), 1408–1412.

Bousquet, L., Lachérade, S., Jacquemoud, S., & Moya, I. (2005). Leaf BRDF measurement and model for specular and diffuse components differentiation. *Remote Sensing of Environment*, *98*(2–3), 201–211.

Bowes, B. G. (1996). *A colour atlas of plant structure* (pp. 97–116). Manson Publishing Ltda.

Brakke, T. (1994). Specular and diffuse components of radiation scattered by leaves. *Agricultural and Forest Meteorology*, *71*, 283–295.

Brakke, T., Otterman, J., Irons, J., & Hall, F. (1996). Assessing canopy biomass and vigor by model-inversion of bidirectional reflectances: Problems and prospects. *16th International geoscience remote sensing symposium — IGARSS'94*, *Vol. 3*. (pp. 1657–1659) Nebraska: Lincoln.

Brakke, T., Smith, J., & Harnden, J. (1989). Bidirectional scattering of light from tree leaves. *Remote Sensing of Environment*, *29*, 175–183.

Breece, H., & Holmes, R. (1971, January). Bidirectional scattering characteristics of healthy green soybean and corn leaves in vivo. *Applied Optics*, *10*(1), 119–127.

Chelle, M. (2003). Could virtual plants be considered as Lambertian objects in dense canopies? In B. -G. Hu & M. Jaeger, (Eds.), *Plant Growth Modeling and Applications — Proceedings of PMA03* (pp. 129-137). Beijing, China: Tsinghua University Press and Springer.

Chelle, M. (2005). Phylloclimate or the climate perceived by individual plant organs: What is it? How to model it? What for? *New Phytologist*, 1–10.

Chiera, J., Thomas, J., & Rufty, T. (2002, March). Leaf initiation and development in soybean under phosphorous stress. *Journal of Experimental Botany*, *53*(368), 473–481.

Clevers, J. (1994). Imaging spectrometry in agriculture — Plant vitality and yield indicators. In J. Hill, & J. Mégier (Eds.), *Imaging spectrometry — a tool for environmental observations* (pp. 193–219). Dordrecht, The Netherlands: Kluwer Academic Publishers.

Davies, A., & Grant, A. (1988). Near infrared spectroscopy for the analysis of specific molecules in food. In C. Creaser, & A. Davies (Eds.), *Analytical applications of spectroscopy* (pp. 46–51). London, Great Britain: Royal Society of Chemistry.

Fourty, T., Baret, F., Jacquemoud, S., Schmuck, G., & Verdebout, J. (1996). Leaf optical properties with explicit description of its biochemical composition: Direct and inverse problems. *Remote Sensing of Environment*, *56*, 104–117.

Ganapol, B., Johnson, L., Hlavka, C., Peterson, D., & Bond, B. (1999). LCM2: A coupled leaf/canopy radiative transfer model. *Remote Sensing of Environment*, *70*, 153–166.

Govaerts, Y., Jacquemoud, S., Verstraete, M., & Ustin, S. (1996, November). Three-dimensional radiation transfer modeling in a dycotyledon leaf. *Applied Optics*, *35*(33), 6585–6598.

Grant, L. (1987). Diffuse and specular characteristics of leaf reflectance. *Remote Sensing of Environment*, *22*, 309–322.

Grant, L., Daughtry, C., & Vanderbilt, V. (1993). Polarized and specular reflectance variance with leaf surface features. *Physiologia Plantarum*, *88*(1), 1–9.

Hobbs, R. (1990). Remote sensing of spatial and temporal dynamics of vegetation. In R. Hobbs, & H. Mooney (Eds.), *Remote sensing of biosphere functioning* (pp. 135–156). New York, USA: Springer Verlag.

Holloway, P. (1982). Structure and histochemistry of plant cuticular membranes: An overview. In D. Cutler, K. Alvin, & C. Price (Eds.), *The plant cuticle. Linnean Society Symposium Series*, *Vol. 10*. (pp. 1–32) London: Academic Press.

Horler, H., & Barber, J. (1981). Principles of remote sensing of plants. In H. Smith (Ed.), *Plants and the daylight spectrum* (pp. 43–64). London: Academic Press.

Horler, H., & Barber, J. (1981). Principles of remote sensing of plants. In H. Smith (Ed.), *Plants and the daylight spectrum* (pp. 43–64). London: Academic Press.

Hosgood, B., Jacquemoud, S., Andreoli, G., Verdebout, J., Pedrini, G., & Schmuck, G. (1995). Leaf optical properties experiment 93. *Tech. Rep. Report EUR 16095 EN*, Joint Research Center, European Comission, Institute for Remote Sensing Applications.

Jacquemoud, S., & Baret, F. (1990). PROSPECT: A model of leaf optical properties spectra. *Remote Sensing of Environment*, *34*(2), 75–92.

Jacquemoud, S., Frangi, J., Govaerts, Y., & Ustin, S. (1997). Three-dimensional representation of leaf anatomy — Application of photon transport. In G. Guyot, & T. Phulpin (Eds.), *7th International symposium of physical measurements and signatures in remote sensing*, *Vol. 1*. (pp. 295–302) Courchevel, France: A.A. Balkema.

Jacquemoud, S., & Ustin, S. (2001). Leaf optical properties: A state of the art. *8th International symposium of physical measurements and signatures in remote sensing* (pp. 223–332). Aussois, France: CNES.

Jacquemoud, S., Ustin, S., Verdebout, J., Schmuck, G., Andreoli, G., & Hosgood, B. (1996). Estimating leaf biochemistry using prospect leaf optical properties model. *Remote Sensing of Environment*, *56*, 194–202.

Johnson, L. (2001). Nitrogen influence on fresh-leaf NIR spectra. *Remote Sensing of Environment*, *78*, 314–320.

Krishnaswamy, A., Baranoski, G., & Rokne, J. G. (2004). Improving the reliability/cost ratio of goniophotometric measurements. *Journal of Graphics Tools*, *9*(3), 31–51.

Maier, S., Lüdeker, W., & Günther, K. (1999). SLOP: A revised version of the stochastic model for leaf optical properties. *Remote Sensing of Environment*, *68*(3), 273–280.

Maracci, G., Schmuck, G., Hosgood, B., & Andreoli, G. (1991). Interpretation of reflectance spectra by plant physiological parameters. *International geoscience and remote sensing symposium — IGARSS'91* (pp. 2303–2306). Finland: Espoo.

Martin, G., Myers, D., & Vogelmann, T. (1991, May). Characterization of plant epidermal lens effects by a surface replica technique. *Journal of Experimental Botany*, *42*(238), 581–587.

Merzlyak, M., O. B., Chivkunova, T. M., & Naqvi, K. (2002). Does a leaf absorb radiation in the near infrared (780–900 nm) region? A new approach to quantifying optical reflection, absorption and transmission leaves. *Photosynthesis Research*, *72*, 263–270.

Nicodemus, F., Richmond, J., Hsia, J., Ginsberg, I., & Limperis, T. (1992). Geometrical considerations and nomenclature for reflectance. In L. Wolff, S. Shafer, & G. Healey (Eds.), *Physics-based vision principles and practice: Radiometry* (pp. 94–145). Boston: Jones and Bartlett Publishers.

Palmer, K., & Williams, D. (1974, August). Optical properties of water in the near infrared. *Journal of the Optical Society of America*, *64*(8), 1107–1110.

Salisbury, F., Dempster, W., Allen, J., Alling, A., Bubenheim, D., Nelson, M., & Silverstone, S. (2002). Light, plants and power for life support on Mars. *Life Support and Biosphere Science*, *8*, 161–172.

Seager, S., Turner, E., Shafer, J., & Ford, E. (2005, June). Vegetation's red edge: A possible spectroscopic biosignature of extraterrestrial plants. *Astrobiology*, *5*(3), 372–390.

Tuchin, V. (2000). *Tissue optics light scattering methods and instruments for medical diagnosis*. Bellingham, WA, USA: The International Society for Optical Engineering.

Tucker, C., & Garratt, M. (1977). Leaf optical system modeled as a stochastic process. *Applied Optics*, *16*(3), 635–642.

Vanderbilt, V. C. (1985, September). Plant canopy specular reflectance model. *IEEE Transactions on Geoscience and Remote Sensing*, *23*(5), 722–730.

Vanderbilt, V., Grant, L., & Ustin, S. (1991). Polarization of light by vegetation. In R. Mynemi, & J. Ross (Eds.), *Photon–vegetation interactions — Applications in optical remote sensing and ecology* (pp. 191–228). Berlin: Springer-Verlag.

Verdebout, J., Jacquemoud, S., & Schmuck, G. (1994). Optical properties of leaves: Modeling and experimental studies. In J. Hill, & J. Mégier (Eds.), *Imaging spectrometry — a tool for environmental observations* (pp. 169–191). Dordrecht, The Netherlands: Kluwer Academic Publishers.

Verstraete, M. (1994). Retrieving canopy properties from remote sensing measurements. In J. Hill, & J. Mégier (Eds.), *Imaging spectrometry — a tool for environmental observations* (pp. 109–123). Dordrecht, The Netherlands: Kluwer Academic Publishers.

Vogelmann, T., & Martin, G. (1993). The functional significance of palisade tissue: Penetration of directional versus diffuse light. *Plant, Cell and Environment*, *16*, 65–72.

Walter-Shea, E., Norman, J., & Blad, B. (1989). Leaf bidirectional reflectance and transmittance in corn and soybean. *Remote Sensing of Environment*, *29*, 161–174.

Weast, R. (1989). *CRC handbook of chemistry and physics*. Boca Raton, Florida, USA: CRC Press.

Wessmann, C. (1990). Evaluation of canopy biochemistry. In R. Hobbs, & H. Mooney (Eds.), *Remote sensing of biosphere functioning* (pp. 135–156). New York, USA: Springer Verlag.

Weyer, L. (1985). Near-infrared spectroscopy of organic substances. *Applied Optics*, *21*(1), 1–43.

Woolley, J. (1971). Reflectance and transmittance of light by leaves. *Plant Physiology*, *47*, 656–662.

Woolley, J. (1973). Change of leaf dimensions and air volume with change in water content. *Plant Physiology*, *41*, 815–816.

Woolley, J. (1975). Refractive index of soybean leaf cell walls. *Plant Physiology*, *55*, 172–174.